Anti-Aβ_{42}– and anti-Aβ_{40}–specific mAbs attenuate amyloid deposition in an Alzheimer disease mouse model

Yona Levites, Pritam Das, Robert W. Price, Marjorie J. Rochette, Lisa A. Kostura, Eileen M. McGowan, Michael P. Murphy, and Todd E. Golde

Department of Neuroscience, Mayo Clinic, Mayo Clinic College of Medicine, Jacksonville, Florida, USA.

Accumulation and aggregation of amyloid β peptide 1–42 (Aβ_{42}) in the brain has been hypothesized as triggering a pathological cascade that causes Alzheimer disease (AD). To determine whether selective targeting of Aβ_{42} versus Aβ_{40} or total Aβ is an effective way to prevent or treat AD, we compared the effects of passive immunization with an anti-Aβ_{42} mAb, an anti-Aβ_{40} mAb, and multiple A$\beta_{1–16}$ mAbs. We established in vivo binding selectivity of the anti-Aβ_{42} and anti-Aβ_{40} mAbs using novel TgBRI-Aβ mice. We then conducted a prevention study in which the anti-Aβ mAbs were administered to young Tg2576 mice, which have no significant Aβ deposition, and therapeutic studies in which mAbs were administered to Tg2576 or CRND8 mice with modest levels of preexisting Aβ deposits. Anti-Aβ_{42}, anti-Aβ_{40}, and anti-A$\beta_{1–16}$ mAbs attenuated plaque deposition in the prevention study. In contrast, anti-Aβ_{42} and anti-Aβ_{40} mAbs were less effective in attenuating Aβ deposition in the therapeutic studies and were not effective in clearing diffuse plaques following direct injection into the cortex. These data suggest that selective targeting of Aβ_{42} or Aβ_{40} may be an effective strategy to prevent amyloid deposition, but may have limited benefit in a therapeutic setting.

Introduction

It is hypothesized that the process whereby amyloid β (Aβ) is accumulated as amyloid triggers the complex pathological changes that ultimately lead to cognitive dysfunction in Alzheimer disease (AD) (1, 2). However, there is substantial debate as to the form or forms of those Aβ aggregates that damage the brain. Aβ accumulates as amyloid in senile plaques and cerebral vessels, but it is also found in diffuse plaques recognized by antibodies but not classic amyloid stains. Although a minor component of the Aβ species produced by processing of amyloid precursor protein (APP), the highly amyloidogenic 42–amino acid form of Aβ (Aβ_{42}) and aminoterminally truncated forms of Aβ_{42} (A$\beta_{x–42}$) are the predominant species of Aβ typically found in both diffuse and senile plaques within the AD brain (3, 4). However many other forms of Aβ (e.g., Aβ_{40} and A$\beta_{x–40}$) are also present, especially in cerebrovascular amyloid deposits (reviewed in ref. 5). Additionally, soluble Aβ aggregates — referred to as oligomers or Aβ-derived diffusible ligands (ADDLs) and able to acutely disrupt neuronal function in rodents — appear to accumulate in the AD brain (6, 7). The exact composition and levels of these oligomers in the brain parenchyma has yet to be elucidated.

The relative levels of Aβ_{42} appear to be the key regulators of Aβ aggregation into amyloid; thus, Aβ_{42} has been implicated as the initiating molecule in the pathogenesis of AD (8). In vitro, Aβ_{42} aggregates into both amyloid fibrils and soluble intermediates more readily than does Aβ_{40} (9). Mutations in the *presenilin* and *APP* genes, which cause early-onset genetic forms of AD, alter Aβ peptide levels predominantly by selectively increasing the relative level of Aβ_{42} and therefore shortening the time to onset of Aβ deposition both in humans and in transgenic animal models (10–12). Finally, more recent studies in mice and *Drosophila* suggest that in the absence of mutations within the Aβ sequence, Aβ_{42} is required for formation of amyloid deposits in vivo (13–15).

Because Aβ_{42} is a minor product of APP metabolism, and because even small shifts in Aβ_{42} production are associated with large effects on Aβ deposition, it has been hypothesized that selective reduction of Aβ_{42} may be an effective way to treat or prevent AD (8, 16). To date, there has been no conclusive experimental evidence to support this hypothesis. The identification of compounds such as certain nonsteroidal antiinflammatory drugs (NSAIDs) that selectively target Aβ_{42} production suggests that it may be possible to pharmacologically target Aβ_{42} in vivo (16, 17). However, the low in vivo potency of these NSAIDs currently limits the conclusions that can be drawn from either clinical or preclinical studies with NSAIDs as they are known to have multiple pharmacologic targets. Thus, in order to explore the utility of selective targeting of Aβ_{42} versus Aβ_{40} or total Aβ, we have examined the effects of passive immunization with an anti-Aβ_{42}–selective mAb and compared the efficacy of this mAb to an anti-Aβ_{40} mAb of the same isotype and 4 anti-A$\beta_{1–16}$ mAbs representing all 4 mouse IgG isotypes. When administered to young mice with minimal Aβ deposition, anti-Aβ_{42}, anti-Aβ_{40}, and anti-A$\beta_{1–16}$ mAbs effectively reduced Aβ accumulation in the brain. However, when administered to older mice with higher Aβ loads, only anti-A$\beta_{1–16}$ mAbs that recognize native Aβ amyloid were effective in attenuating Ab deposition.

Nonstandard abbreviations used: Aβ, amyloid β; Ab2, anti-A$\beta_{1–16}$ mAb of IgG3 isotype; Ab3, anti-A$\beta_{1–16}$ mAb of IgG1 isotype; Ab5, anti-A$\beta_{1–16}$ mAb of IgG2b isotype; Ab9, anti-A$\beta_{1–16}$ mAb of IgG2a isotype; Ab40.1, anti-Aβ_{40} mAb; Ab42.2, anti-Aβ_{42} mAb; AD, Alzheimer disease; APP, amyloid precursor protein; CAA, cerebral amyloid angiopathy; FA, formic acid; FA Aβ, Aβ level measured by ELISA following FA extraction; FcR, Fc receptor; NSAID, nonsteroidal antiinflammatory drug; SDS Aβ, Aβ level measured by ELISA following SDS extraction.

Conflict of interest: The authors have declared that no conflict of interest exists.

Citation for this article: *J. Clin. Invest.* **116**:193–201 (2006). doi:10.1172/JCI25410.

Table 1
Antibodies used for passive immunization

mAb	Immunogen	Isotype	Epitope[A]	Plaque binding[B]	Specificity[C]
Ab42.2	$A\beta_{35-42}$	IgG1	$A\beta_{x-42}$	–	<0.1%
Ab40.1	$A\beta_{35-40}$	IgG1	$A\beta_{x-40}$	–	<0.1%
Ab2	$fA\beta_{1-42}$[D]	IgG3	$A\beta_{1-16}$	+	Pan-Aβ
Ab3	$A\beta_{1-16}$	IgG1	$A\beta_{1-16}$	+++	Pan-Aβ
Ab5	$fA\beta_{1-42}$[D]	IgG2b	$A\beta_{1-16}$	++	Pan-Aβ
Ab9	$fA\beta_{1-42}$	IgG2a	$A\beta_{1-16}$	+++	Pan-Aβ

[A]Epitope mapping using various Aβ peptides was performed on each mAb. [B]The ability of the mAb to bind plaques was assessed by staining cryostat sections from unfixed frozen human AD hippocampus: +++, full stain; ++, partial stain; +, marginal stain; –, no stain (see Methods). [C]Binding to serial dilutions of $A\beta_{40}$, $A\beta_{42}$, and $A\beta_{38}$ was used to determine the crossreactivity of Ab42.2 and Ab40.1 by capture ELISA. [D]Immunogen used was aggregated $A\beta_{1-42}$. fAβ, fibrillar Aβ.

Results

Selective in vivo binding by anti-$A\beta_{42}$ and anti-$A\beta_{40}$ mAbs. We have generated and characterized multiple anti-Aβ mAbs (Table 1). Based on in vitro ELISA analysis of their binding properties, both the anti-$A\beta_{42}$ mAb (Ab42.2) and the anti-$A\beta_{40}$ mAb (Ab40.1) were highly selective for $A\beta_{x-42}$ and $A\beta_{x-40}$, respectively, whereas the mAbs that recognize the NH_2-terminal epitope of Aβ ($A\beta_{1-16}$) bound both $A\beta_{40}$ and $A\beta_{42}$ as well as other Aβ peptides (e.g., $A\beta_{37}$, $A\beta_{38}$, and $A\beta_{39}$; Figure 1, A and B). To determine whether these mAbs maintain their selectivity for specific Aβ species in vivo, we used novel transgenic BRI-Aβ (TgBRI-Aβ) mice that selectively express either $A\beta_{1-40}$ (TgBRI-$A\beta_{40}$) or $A\beta_{1-42}$ (TgBRI-$A\beta_{42}$). In these TgBRI-Aβ mice, Aβ can be detected both in the brain and in plasma (13).To evaluate in vivo binding of these mAbs in TgBRI-Aβ mice, biotinylated Ab42.2, Ab40.1, or the anti-$A\beta_{1-16}$ mAb of the IgG2a isotype (Ab9) were injected i.p., and biotinylated mAb–Aβ complexes were detected using a modified sandwich ELISA protocol (Figure 1, C and D). Biotinylated Ab9–Aβ complexes were detected in the plasma of both TgBRI-$A\beta_{40}$ and TgBRI-$A\beta_{42}$ mice. Biotinylated Ab42.2–Aβ complexes were detected only in plasma from TgBRI-$A\beta_{42}$ mice and not in TgBRI-$A\beta_{40}$ mice, whereas biotinylated Ab40.1–Aβ complexes were detected only in TgBRI-$A\beta_{40}$ mice and not in TgBRI-$A\beta_{42}$ mice. No signal was detected in nontransgenic mice injected with any of these biotinylated mAbs (data not shown). These data provide strong support for in vivo specificity of Ab42.2 and Ab40.1 by demonstrating that they selectively bind their target Aβ species in vivo.

Passive immunotherapy with anti-$A\beta_{42}$– and anti-$A\beta_{40}$–specific mAbs attenuates amyloid deposition in young Tg2576 mice. Having established the in vivo binding specificity of Ab42.2, Ab40.1, and Ab9, we tested the effect of peripheral administration of these mAbs on Aβ deposition in Tg2576 mice (18). Two studies were performed: a prevention study, in which the anti-Aβ mAbs were administered to 7-month-old female Tg2576 mice, which have minimal Aβ deposition, and a therapeutic study, in which the mAbs were administered to 11-month-old Tg2576 mice, which have moderate levels of preexisting Aβ deposits (19). Biochemical and immunohistochemical methods were used to analyze the effect of passive immunization on Aβ deposition (Figure 2). After 4 months of passive immunization with Ab9, Ab42.2, and Ab40.1, initiated when the mice were 7 months old, Aβ levels were significantly attenuated as assessed biochemically with Aβ ELISA following SDS extraction (>50% reduction in SDS Aβ; Figure 2A) or formic acid (FA) extraction of the SDS-insoluble material (>50% reduction in FA Aβ; Figure 2B). Figure 2C shows representative immunostained sections from immunized and control Tg2576 mice. Quantitative analysis of multiple immunostained sections also revealed a significant decrease in Aβ deposition. Both plaque numbers per field (Figure 2D) and total immunoreactive plaque load (data not shown) were significantly reduced. The ratio between $A\beta_{42}$ and $A\beta_{40}$ was not significantly altered in either Ab42.2- or Ab40.1-treated mice (data not shown). In contrast, 4 months of passive immunization with these same

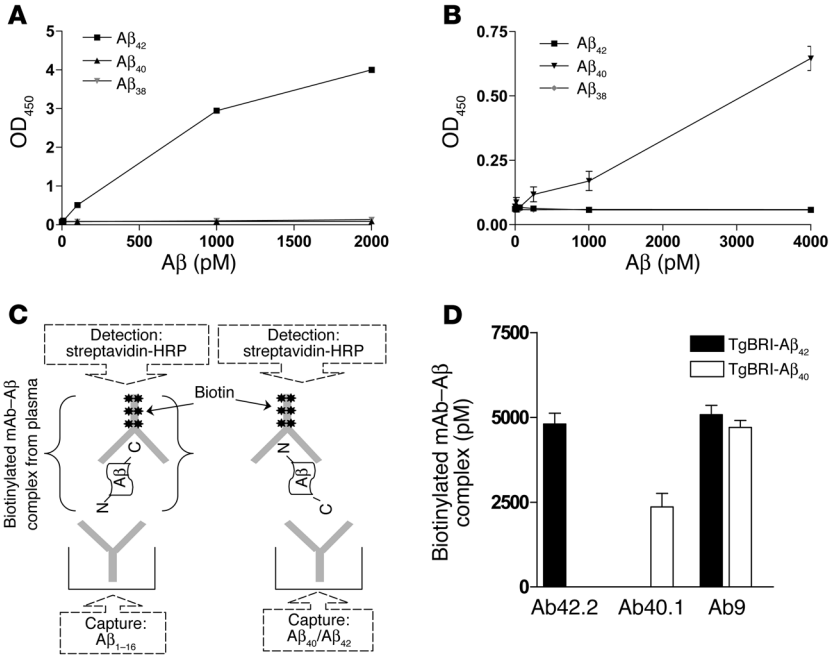

Figure 1
Specificity of Ab40.1 and Ab42.2. (**A**) Serial dilutions of $A\beta_{40}$, $A\beta_{42}$, and $A\beta_{38}$ were used to determine the crossreactivity of Ab42.2 by capture ELISA. Ab42.2 was used as capture and Ab9-HRP as detection. (**B**) Serial dilutions of $A\beta_{40}$, $A\beta_{42}$, and $A\beta_{38}$ were used to determine the crossreactivity of Ab40.1 by capture ELISA. Ab9 was used as capture and Ab40.1 as detection. (**C**) Schematic depicting the method for capture ELISA of biotinylated mAb–Aβ complexes in plasma. (**D**) Specificity of Ab42.2 and Ab40.1 in vivo. Biotinylated Ab42.2, Ab40.1, and Ab9 (500 μg) were injected i.p. into TgBRI-$A\beta_{40}$ and TgBRI-$A\beta_{42}$ mice (n = 3 per group). Seventy-two hours after injection, levels of biotinylated mAb–Aβ complexes in plasma were determined using capture ELISA as illustrated in **C**. Plasma levels of $A\beta_{40}$ were ~1000 pM in TgBRI-$A\beta_{40}$ mice, and plasma $A\beta_{42}$ levels were ~1000 pM in TgBRI-$A\beta_{42}$ mice. No $A\beta_{42}$ was detected in the plasma of TgBRI-$A\beta_{40}$ mice, and no $A\beta_{40}$ was detected in the plasma of TgBRI-$A\beta_{42}$ mice.

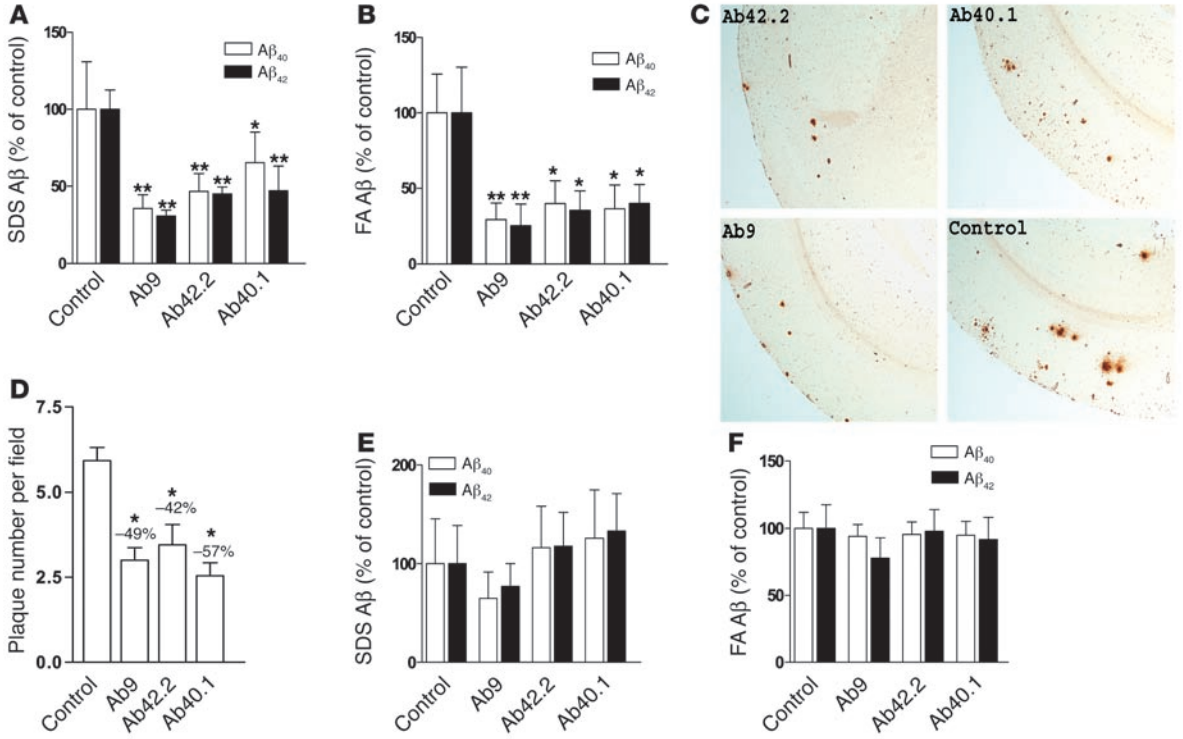

Figure 2

Effect of immunization with C-terminal–specific mAbs on Aβ levels in brains of Tg2576 mice. (**A** and **B**) Seven-month-old Tg2576 mice ($n = 6$ per group) were immunized with 500 μg of Ab40.1 and Ab42.2 biweekly for 4 months, and Aβ levels were compared with those following immunization with Ab9. Control mice received PBS. Mice were killed following treatment, and both SDS Aβ (**A**) and FA Aβ (**B**) were analyzed by capture ELISA. SDS $A\beta_{40}$ and FA $A\beta_{40}$ in control mice were 123 ± 27 and 3,613 ± 610 pmol/g, respectively; SDS $A\beta_{42}$ and FA $A\beta_{42}$ in control mice were 44 ± 4 and 840 ± 180 pmol/g, respectively. (**C**) Representative immunostained sections for amyloid plaques from brains of mAb-immunized 7-month-old Tg2576 mice. Magnification, ×100. (**D**) Quantitative image analysis of amyloid plaque burden in the neocortices of immunized 7-month-old Tg2576 mice. (**E** and **F**) Eleven-month-old Tg2576 mice ($n = 6$ per group) were immunized with Ab40.1, Ab42.2, and Ab9 biweekly for 4 months. SDS Aβ (**E**) and FA Aβ (**F**) were analyzed by capture ELISA. SDS $A\beta_{40}$ and FA $A\beta_{40}$ in control mice were 1,115 ± 72 and 4,675 ± 430 pmol/g, respectively; SDS $A\beta_{42}$ and FA $A\beta_{42}$ in control mice were 348 ± 34 and 737 ± 62 pmol/g, respectively. $^*P < 0.05$, $^{**}P < 0.01$ vs. control.

mAbs, initiated when the Tg2576 mice were 11 months old, had no significant effect on biochemical (Figure 2, E and F) or immunohistochemical Aβ loads (data not shown), although a slight but nonsignificant decrease in the SDS Aβ was seen in the Ab9-treated animals (35% reduction in SDS Aβ; Figure 2E).

To further examine the relative efficacy of these anti-Aβ mAbs in altering Aβ accumulation, we passively immunized CRND8 mice. This transgenic model has a very early onset of Aβ deposition, both as amyloid and in more diffuse plaques. Furthermore, compared with Tg2576 mice, the relative level of $A\beta_{42}$ is much higher than that of $A\beta_{40}$ (20). Thus, in CRND8 mice, as in most cases of AD, the predominant species deposited is $A\beta_{42}$. In contrast, $A\beta_{40}$ is the predominant species deposited in Tg2576 mice. At 3 months of age, CRND8 mice have amyloid pathology roughly comparable to that of 10-month-old Tg2576 mice (21). Weekly injections of 3-month-old CRND8 mice with 500 μg of Ab9 and Ab42.2 mAbs for 8 weeks resulted in significant reduction of SDS Aβ but not FA Aβ only in Ab9-treated mice (>40% reduction in SDS Aβ; Figure 3, A and B). Total $A\beta_{42}$ levels (SDS Aβ plus FA Aβ) were also significantly reduced by Ab9 treatment. Quantitative analysis of the immunostained sections also revealed a significant decrease in Aβ deposition in Ab9-treated mice (Figure 3, C and D). Immunization with Ab42.2 did not lead to a significant decrease in Aβ load, although there was a trend toward reduction in $A\beta_{42}$ levels ($P = 0.13$), suggesting that this mAb is less effective than Ab9 in clearing amyloid deposits in CRND8.

Effects on cerebral amyloid angiopathy and related microhemorrhage. Wilcock et al. (22) show that passive immunization increases amounts of vascular amyloid staining in very old Tg2576 mice. To examine the effect of passive immunization on cerebral amyloid angiopathy (CAA) in our models, brain sections were stained with biotinylated Ab9. Vessels with detectable CAA were divided into 3 groups based on the extent of CAA within each vessel (as visualized by immunostaining; see Methods) and the number of vessels with any degree of CAA counted in 5–10 sections per mouse. In Tg2576 mice and CRND8 mice, CAA was mostly associated with areas rich in amyloid plaques (Table 2), a result consistent with recent findings (23). In 7-month-old Tg2576 mice immunized with anti-Aβ mAbs, few blood vessels with trace amounts of Aβ amyloid staining were detected in control mice, but none were detected in the immunized mice with decreased levels of amyloid in the brain. Similarly, in the passively immunized CRND8 mice, the number and the intensity of CAA-positive vessels were slightly but not significantly reduced (Table 2). The Tg2576 mice in the

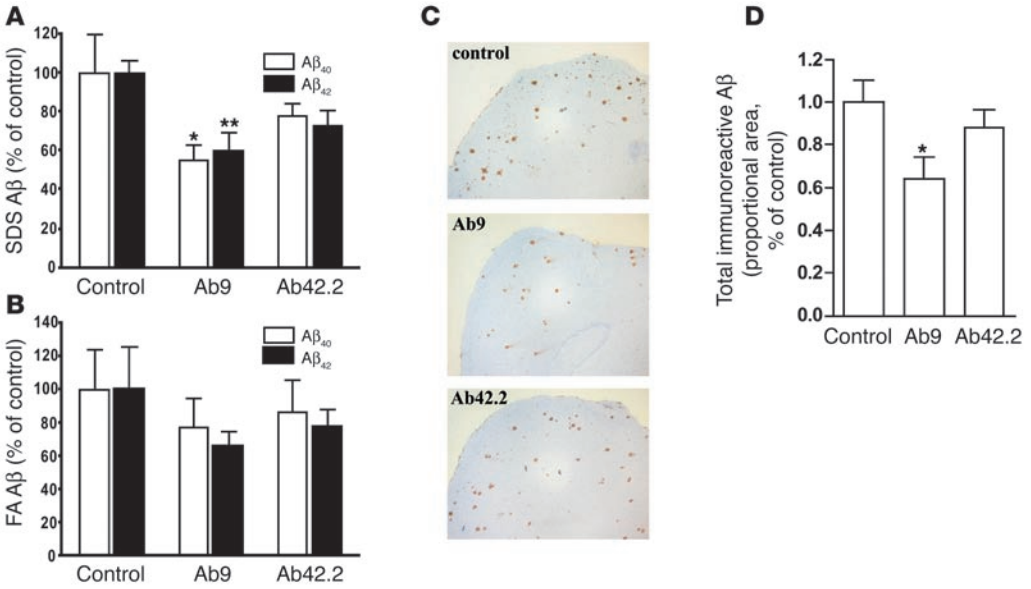

Figure 3
Effect of immunization with anti-Aβ mAbs on Aβ levels in brains of CRND8 mice. (**A** and **B**) Three-month-old CRND8 mice ($n = 6$ per group) were immunized with 500 μg of Ab9 or Ab42.2 weekly for 8 weeks. Control mice received PBS. Mice were killed following treatment, and both SDS Aβ (**A**) and FA Aβ (**B**) fractions were analyzed by capture ELISA. SDS $Aβ_{40}$ and FA $Aβ_{40}$ in control mice were 217 ± 40 and 563 ± 95 pmol/g, respectively; SDS $Aβ_{42}$ and FA $Aβ_{42}$ in control mice were 189 ± 12 and 636 ± 51 pmol/g, respectively. (**C**) Representative immunostained sections for amyloid plaques from brains of mAb-immunized CRND8 mice. Magnification, ×40. (**D**) Quantitative image analysis of amyloid plaque burden in the neocortices of immunized CRND8 mice. *$P < 0.05$, **$P < 0.01$ vs. control.

therapeutic study had extensive CAA in the neocortex. Following immunization, there was no appreciable difference in the extent of CAA between control and treated mice. Passive immunization with mAbs directed against the NH_2 terminus of Aβ has recently been reported to exacerbate CAA-related microhemorrhage in PDAPP and APP23 transgenic mice (24, 25). Using both Perls stain and H&E to visualize microhemorrhages, we did not find any evidence for appreciable levels of microhemorrhage in the control Tg2576 and CRND8 mice (less than 1 microhemorrhage event per brain section), nor was there a detectable increase in microhemorrhage following mAb administration (data not shown).

Direct cortical injections of anti-Aβ mAbs. To further explore the ability of the mAbs to alter plaque deposition, we examined the effects of direct intracortical injections of Ab40.1 and Ab42.2 as well as multiple anti-$Aβ_{1–16}$ mAbs into 18-month-old Tg2576 mice. In each case, 72 hours after cortical injection, the mice were killed, and the immunostained plaque load and thioflavin-S–positive plaque load was determined in the immediate vicinity of the injection site. Immunostained plaque load of Aβ was significantly decreased by Ab9, anti-$Aβ_{1–16}$ mAb of IgG1 isotype (Ab3), and anti-$Aβ_{1–16}$ mAb of IgG3 isotype (Ab2), whereas the anti-$Aβ_{1–16}$ mAb of IgG2b isotype (Ab5) and both Ab40.1 and Ab42.2 had no measurable effect (Figure 4, A and C). In contrast, thioflavin-S staining of adjacent serial sections showed no effect on dense-cored plaque loads by any mAb (Figure 4, B and D), suggesting that only diffuse Aβ deposits were selectively cleared by certain anti-$Aβ_{1–16}$ mAbs. To confirm that control mouse IgG did not have any effect on plaque load, we extensively compared plaque load in control IgG–treated sections with plaque load in the contralateral noninjected areas and found no significant difference between them (data not shown).

Binding of mAbs to plaques correlates well with their ability to alter Aβ deposition in mice with preexisting Aβ deposits. In order to further characterize the properties of these mAbs associated with the ability to apparently clear preexisting diffuse Aβ deposits, we performed 2 additional studies. First, we compared the relative affinity of these mAbs for binding to native unfixed plaques using frozen unfixed AD brain sections (Figure 5A). These data show that Ab40.1 and Ab42.2 did not bind native plaques, whereas all of the anti-$Aβ_{1–16}$ mAbs showed significant binding (Figure 5A). Quantification of the fluorescence intensity per plaque did reveal that there were differences in the relative affin-

Table 2
Effect of immunotherapy on the number of CAA-positive blood vessels in the neocortices of Tg2576 and CRND8 mice

		No. immunostained vessels[A]		
		+++	++	+
Tg2576 (preventative)	Control	0	0	2.4 ± 0.5
	Ab9	0	0	0
	Ab42.2	0	0	0
CRND8 (therapeutic)	Control	7 ± 0.8	4.4 ± 0.5	3.2 ± 0.9
	Ab9	4.3 ± 0.5[B]	4 ± 0.9	2.7 ± 0.9
	Ab42.2	6.3 ± 0.3	6 ± 0.9	4.3 ± 0.6
Tg2576 (therapeutic)	Control	3 ± 0.3	5.2 ± 1.6	6.3 ± 3.2
	Ab9	2.6 ± 0.3	4.3 ± 1.9	7.2 ± 2.1
	Ab42.2	2.8 ± 0.4	4.6 ± 1.3	7.8 ± 2.6

Mice were categorized as follows: +++, full stain; ++, partial stain; +, marginal stain (see Methods). [A]Values given are based on 5–10 sections per mouse. [B]$P < 0.05$ vs. control.

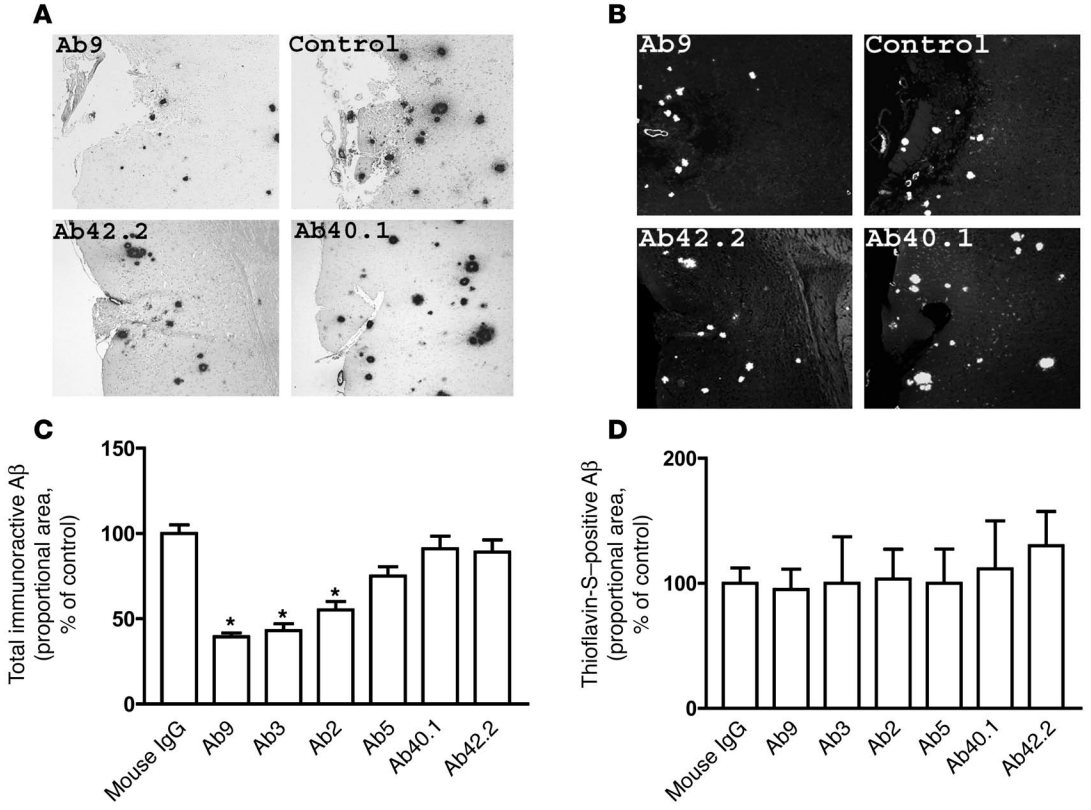

Figure 4
Effect of direct cortical injections with anti-Aβ mAbs on Aβ plaque burdens in 18-month-old Tg2576 mice. Mice were injected in the frontal cortex with 1 μg each the following mAbs: control mouse IgG, Ab2, Ab3, Ab5, Ab9, Ab40.1, and Ab42.2. (**A**) Representative images of immunostained Aβ plaques taken from injection sites in cortex following injection with Ab9, control IgG, Ab42.2, and Ab40.1. (**B**) Representative images of thioflavin-S–positive Aβ plaques taken from injection sites in cortex following injection with Ab9, control IgG, Ab42.2, and Ab40.1. Magnification, ×100. (**C**) Quantitative analysis of immunostained amyloid plaque burdens in mice following mAb injections. *$P < 0.01$ vs. mouse IgG. (**D**) Quantitative analysis of thioflavin-S–positive amyloid plaque burdens in mice following mAb injections.

ity for plaques based on this assay among the anti-$A\beta_{1-16}$ mAbs (in descending order of affinity, Ab9 and Ab3, Ab5, and Ab2; Figure 5B). Though neither Ab40.1 nor Ab42.2 bound plaques in this assay, both mAbs did bind plaques following FA treatment of formalin-fixed sections (data not shown).

Previous reports have implicated both native plaque binding and isotype as important determinants that correlated with efficacy of passive immunization with anti-Aβ mAbs (26); therefore, we compared the effect of each of our anti-$A\beta_{1-16}$ mAbs on Aβ deposition in Tg2576 mice. As noted above, these mAbs differ in their ability to recognize native amyloid plaques but also encompass each of the 4 mouse IgG isotypes. In this study, immunization was initiated using 10-month-old Tg2576 mice and continued for 4 months. At sacrifice, biochemical Aβ loads were analyzed. Immunization with each mAb reduced SDS Aβ (Figure 5C). SDS $A\beta_{40}$ was significantly reduced by Ab9 and Ab3, and SDS $A\beta_{42}$ was significantly reduced by Ab9, Ab3, and Ab5. Similarly, FA Aβ was also reduced by each mAb (Figure 5D). Ab9 and Ab3 treatment resulted in significant reductions in both FA $A\beta_{40}$ and FA $A\beta_{42}$, whereas only the reduction in FA $A\beta_{40}$ was significantly attenuated by Ab5. In this study, the rank order of efficacy of these 4 mAbs as passive immunogens correlated with their rank order in terms of plaque binding (in descending order of efficacy, Ab9 and Ab3, Ab5, and Ab2).

Discussion

Our data provide an initial proof-of-concept study demonstrating that selective targeting of Aβ with mAbs that selectively bind either $A\beta_{42}$ or $A\beta_{40}$ in vitro and in vivo attenuate Aβ deposition when administered to APP Tg2576 mice prior to significant Aβ deposition. These data are similar to results presented in a recently published study in Tg2576 mice immunized with the anti-$A\beta_{42}$ mAb BC05 prior to onset of deposition (26); however, in that report, in vivo specificity of the anti-$A\beta_{42}$ mAb was not directly assessed. As it is generally hypothesized that amyloid deposition precedes cognitive impairment by many years and that $A\beta_{42}$ initiates amyloid deposition, our data provide evidence in support of preventative pharmacologic or antibody-based therapies that selectively target $A\beta_{42}$ prior to the onset of AD. Ab42.2 treatment did not alter Aβ deposition when administered to Tg2576 mice with modest plaque loads, did not clear deposited Aβ following direct cortical injection, and only slightly attenuated deposition when administered to CRND8 mice with modest amyloid loads at the initiation of treatment. These later findings are similar to a report with a different anti-$A\beta_{42}$ mAb, which had no effect on deposition following passive immunization in the PDAPP transgenic mouse model (27). Thus, consistent with earlier results using active immunization in Tg2576 mice (28), we found that passive immunization with mAbs was less effective when treatment was initiated after the onset of

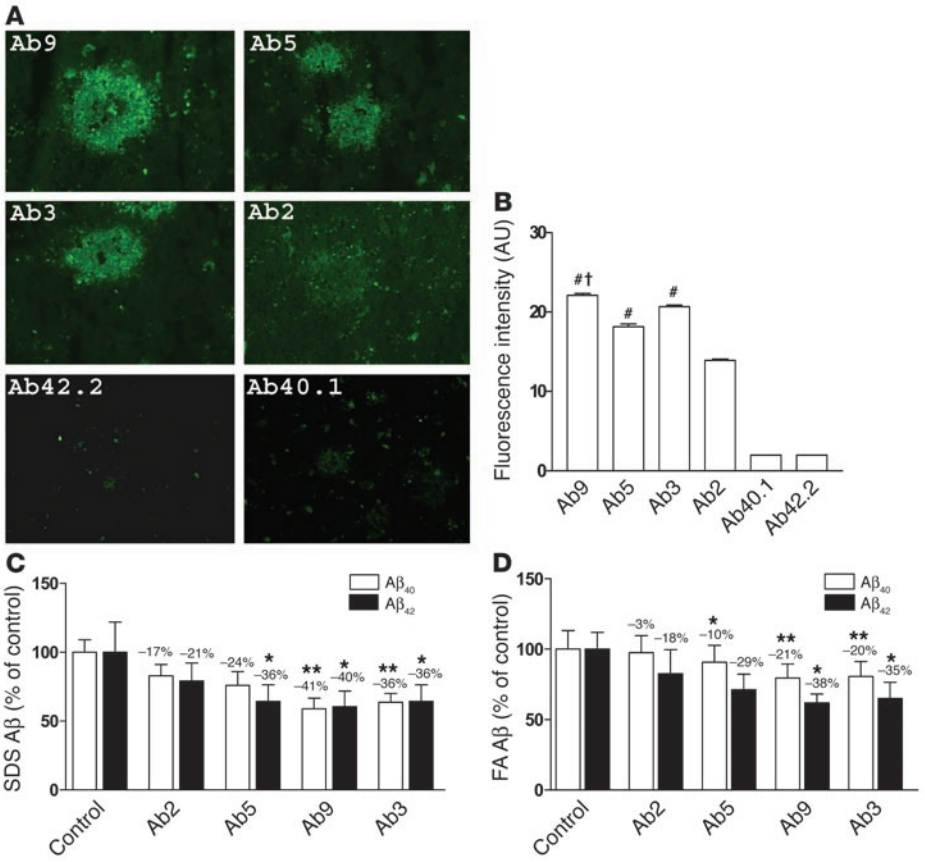

Figure 5
Effect of immunization with N-terminal–specific mAbs on Aβ levels in brains of 10-month-old Tg2576 mice. (**A**) Unfixed, frozen cryostat serial sections of human AD tissue (hippocampus) were stained with Ab9, Ab5, Ab3, Ab2, Ab40.1, and Ab42.2. Representative plaque staining is shown. Magnification, ×400. (**B**) Quantitative image analysis of the average fluorescence intensity level per plaque following mAb binding. $^{\#}P < 0.001$ vs. Ab40.1; $^{\dagger}P < 0.05$ vs. Ab2. (**C** and **D**) Aβ levels in brains of Ab2-, Ab5-, Ab9-, and Ab3-immunized Tg2576 mice. Ten-month-old Tg2576 mice ($n = 6$ per group) were immunized biweekly with 500 μg N-terminal mAbs for 4 months. Mice were sacrificed following treatment, and brain tissue was subject to a 2-step SDS or FA extraction. Both SDS Aβ (**C**) and FA Aβ (**D**) were analyzed by capture ELISA. SDS $Aβ_{40}$ and FA $Aβ_{40}$ in control mice were 1,115 ± 72 and 4,675 ± 430 pmol/g, respectively; SDS $Aβ_{42}$ and FA $Aβ_{42}$ in control mice were 348 ± 54 and 737 ± 62 pmol/g, respectively. $^{*}P < 0.05$, $^{**}P < 0.01$ vs. control.

Aβ deposition, data that reinforce the concept that it may be easier to prevent Aβ deposition than to alter it once deposited. We also found that an anti-$Aβ_{40}$ mAb that shows selectivity for $Aβ_{40}$ in vitro and in vivo had effects indistinguishable from those of the anti-$Aβ_{42}$ mAb, showing efficacy in a prevention study but not in a therapeutic study. A previous study has reported that an anti-$Aβ_{40}$ mAb is a highly effective passive immunogen in Tg2576 and Tg2576 × *PS1*mt mice (a transgenic progeny from a cross between the Tg2576 line and a mutant $PS1_{M46L}$ line); however, no data regarding the specificity of that mAb was provided (22).

Despite the multiple studies examining various parameters that may predict the efficacy of anti-Aβ immunotherapy in mice, there is no consensus on how anti-Aβ immunotherapy works (29–37). Our data show that the extent of Aβ deposition prior to initiation of immunization experiments influences efficacy, and, depending on the amount of Aβ present when immunization is initiated, different properties of the mAbs can affect the outcome. Such data provide further support for the hypothesis that anti-Aβ mAbs alter Aβ deposition through multiple mechanisms. It is also likely that the efficacy of anti-Aβ immunization depends on the type of Aβ deposits present in the APP mouse model being tested (38). In Tg2576 mice, the majority of Aβ is deposited as dense-cored, thioflavin-S–positive plaques; only in very old animals (>15 months) does an appreciable amount of diffuse Aβ deposits appear (19). In Tg2576 mice, we have no convincing evidence to date that the dense-cored plaques are being cleared by mAbs, even when the mAb is applied directly to the brain, although direct application did clear diffuse deposits of Aβ. Thus, we interpret our peripheral passive immunization data as being more consistent with preventing additional plaque deposition than with clearing existing plaques. Data from other groups do show that clearance can occur; in many but not all of these cases, the difference in results may be attributable to the greater amounts of diffuse deposits in the APP mouse models used (22, 32, 38–40). In any case, it is likely that the preponderance of dense-cored plaques and their relative resistance to immune clearance can account for the difference in the magnitude of the effect we observed compared with reports by others in mice with more diffuse plaques that may be cleared more effectively (e.g., PDAPP, APP × PS1mt, 3×-Tg–AD) (22, 28, 32, 40).

In the prevention studies, where treatment was initiated prior to significant plaque deposition, selective targeting of $Aβ_{42}$ or $Aβ_{40}$ with end-specific mAbs and nonselective targeting of Aβ with anti-$Aβ_{1–16}$ mAbs were equally effective at reducing plaque deposition. Surprisingly, there was no significant difference in the ratio of $Aβ_{40}$ to $Aβ_{42}$ deposited following administration of these mAbs. If the end-specific mAbs were working by only targeting individual Aβ species, one might expect to see alterations in the ratio of deposited Aβ. The lack of effect on the ratio of deposited Aβ may be attributable to targeting or disruption of an early aggregation intermediate formed by $Aβ_{40}$ and $Aβ_{42}$, capping of growth of fibrils composed of both $Aβ_{40}$ and $Aβ_{42}$, or the mAb triggering some clearance mechanisms that alter deposition of both species.

When immunization was initiated in mice with significant preexisting plaque loads, we found that the efficacy of immunization with any type of mAb was reduced. The end-specific mAbs were less effective than pan-Aβ mAbs in the therapeutic regimen. In order to have efficacy in these therapeutic types of studies, it

appears that the mAb must be capable of recognizing Aβ deposited as amyloid plaques. Similar correlations have been previously reported (26, 38, 41), and even in the human trial a correlation between plaque binding and cognitive improvement was reported in a small subset of patients receiving the AN-1792 vaccine (42, 43). Indeed, one might predict from the deduced structure of Aβ amyloid that the COOH-terminal epitopes are buried in the fibril and inaccessible to an antibody, whereas aminoterminal epitopes are more accessible (44).

A previous study in PDAPP mice demonstrated that the most effective passive immunogens of the panel of mAbs binding in the NH_2 terminus of Aβ that were tested were 2 mAbs of the IgG2a isotype (27). These data, and the presence of Aβ-laden microglia observed in certain active and passive immunization paradigms, have been used to support the hypothesis that Fc receptor–mediated (FcR-mediated) uptake of Aβ by microglia maybe a key mechanism underlying efficacy of anti-Aβ immunotherapy (32, 41, 45, 46). In contrast, our current and previous results in Tg2576 mice do not support a major role for FcR-mediated uptake by microglia in mediating the efficacy of anti-Aβ immunotherapy (1). Similarly, other studies suggest that FcR-mediated uptake of anti-Aβ mAbs is not required for clearance of Aβ (47, 48). Entirely consistent with our previous data in FcRγ knockout mice, we found that Ab3, which has low affinity for FcR, and Ab9, which has high affinity for FcR (49), were equally effective in attenuating Aβ deposition in passive immunization studies initiated in 10-month-old Tg2576 mice and effectively cleared plaques when injected directly into the cortices of mice. Similarly, both end-specific mAbs used in this study were IgG1, suggesting that their mechanism of action does not depend on FcR. At least 1 other group has reported that intracerebroventricular administration of an IgG1 anti-Aβ mAb recognizing the NH_2 terminus of Aβ was effective at clearing Aβ (48).

Several recent studies showed that passive Aβ immunization induces an increase in cerebral microhemorrhage associated with amyloid-laden vessels (24, 25) as well as an increase in amounts of vascular amyloid staining (22). A semiquantitative assessment of CAA in the Tg2576 and CRND8 mice in this study showed that a reduction in amyloid loads caused by passive immunization with anti-Aβ mAbs resulted in a decrease in the number of CAA-positive blood vessels. Furthermore, no evidence for CAA-resulting microhemorrhage was observed. Our negative data should be interpreted cautiously. There are simply too many differences in the models and mAbs used to conclude that the lack of effect on CAA and microhemorrhage we observed is related to the mAb used. In any case we suggest that both of these possible side effects of passive immunotherapy would be minimized if the treatment were begun prior to significant amyloid deposition.

Despite the halting of the phase II human clinical trial of active $Aβ_{42}$ immunization due to a meningioencephalitic presentation in approximately 5% of vaccinated individuals (45, 50), anti-Aβ immunotherapy remains a very promising therapeutic approach for the treatment or prevention of AD. By selectively targeting the most pathogenic form of Aβ, an end-specific mAb targeting $Aβ_{42}$ may have some safety advantages over other anti-Aβ mAbs. Such end-specific mAbs do not bind to the APP or other fragments derived by proteolysis of APP and may be less likely to interact with vascular amyloid that predominantly consists of $Aβ_{40}$ (3, 4). Moreover, because $Aβ_{42}$ is a minor Aβ species, lower mAb amounts may be needed to have a beneficial effect.

Methods

Antibodies. The mAbs used for immunizations are shown in Table 1. The mAbs were generated at Mayo Clinic Monoclonal Antibody Core Facilities as follows: Culture supernatants of hybridoma cells were screened for binding to Aβ immunogens by ELISA. Positive clones were then grown in suspension in DMEM, supplemented with 10% FCS Clone I and 1 mg/ml IL-6. Secreted mAbs were purified using Protein G columns (Invitrogen Corp.) and then used for all experiments. Mouse IgG was purchased from Equitech-Bio Inc.

Mice. All animal husbandry procedures performed were approved by Mayo Clinic Institutional Animal Care and Use Committee in accordance with NIH guidelines under protocol A34602. Tg2576 mice (B6/SJL) were produced as described previously (18) and were obtained from Charles River Laboratories. To generate CRND8 mice, male CRND8 mice containing a double mutation in the human APP gene (K670M/N671L and V717F) (21) were mated with female B6C3F1/Tac mice obtained from Taconic. Genotyping of Tg2576 and CRND8 mice was performed by PCR as described previously (18, 21). All animals were housed 3–5 to a cage and maintained on ad libitum food and water with a 12-hour light/dark cycle.

Capture ELISA for comparison of crossreactivity of end-specific mAbs. Serial dilutions of $Aβ_{40}$ and $Aβ_{42}$ were used to determine the crossreactivity of Ab40.1 and Ab42.2. Ab9 was used as capture and Ab40.1-HRP as detection, or Ab42.2 as capture and Ab9-HRP as detection.

Measurement of mAb-Aβ complex in plasma. To measure the biotinylated mAb–Aβ complex in the plasma, TgBRI-$Aβ_{40}$ and TgBRI-$Aβ_{42}$ mice (13) were immunized with 500 μg biotinylated mAb i.p., and plasma was collected 72 hours later. We used an mAb against the free end of Aβ peptide as capture and streptavidin-HRP as detection (Figure 1C).

Staining of lightly fixed Aβ plaques. Cryostat sections (10 μm) from frozen, unfixed human AD tissue (hippocampus) were lightly fixed in cold acetone for 2 minutes, blocked with 1% normal goat serum for 1 hour, and incubated with Ab9, Ab3, Ab2, or Ab5, each at 1 μg/ml, for 2 hours at room temperature. Slides were then washed in PBS, incubated with goat anti-mouse conjugated to Alexa Fluor 488 (1:1000; Invitrogen Corp.) for 1 hour, washed, and mounted. For quantification of fluorescence, images of at least 3–5 randomly selected fields of plaques were obtained, and fluorescence intensity levels on individual plaques were measured using Analytical Imaging System (AIS, version 4.0; Imaging Research Inc.). The average fluorescence intensity level per plaque was determined by dividing the sum of the fluorescence intensity of plaques by the total number of plaques analyzed (total of 10–15 plaques of equal size per group were used).

Passive immunizations. Groups of Tg2576 mice (females, 7, 10, or 11 months old, $n = 6$ per group) were immunized i.p. with 500 μg of mAb once every 2 weeks for 4 months. CRND8 mice (females, 3 months old, $n = 7$ per group) were immunized i.p. with 500 μg of mAb once every week for 8 weeks. Control mice received mouse IgG or PBS.

Cortical injections. For stereotaxic cortical injections, Tg2576 mice (females, 18 months old, $n = 3$ per group) mice were injected with 1 μg of mAb in the frontal cortex of the right hemisphere, whereas the left hemisphere was left untreated as a control. On the day of the surgery, mice were anesthetized with isoflurane (5% initially followed by 3% during surgery) and placed in a stereotaxic apparatus. A midsagittal incision was made to expose the cranium, and a hole was drilled to the following coordinates taken from bregma: A/P, +1.1 mm; L, –1.5 mm. A 26-gauge needle attached to a 10-μl syringe was lowered 1.0 mm dorsoventral, and a 2-μl injection was made over a 10-minute period. The incision was closed with surgical staples, and mice were sacrificed 72 hours after the surgery.

ELISA analysis of extracted Aβ. At sacrifice, the brains of mice were divided by midsagittal dissection, and 1 hemibrain was used for biochemical analysis. Each hemibrain was sequentially extracted in a 2-step procedure

described previously (19). Briefly, each hemibrain (150 mg/ml wet wt) was sonicated in 2% SDS with protease inhibitors and centrifuged at 100,000 *g* for 1 hour at 4°C. Following centrifugation, the resultant supernatant was collected, representing the SDS-soluble fraction. The resultant pellet was then extracted in 70% FA, centrifuged, and the resultant supernatant collected (the FA fraction). The following mAbs against Aβ were used in the sandwich capture ELISA: for brain $Aβ_{40}$, Ab9 capture and Ab40.1-HRP detection; for brain $Aβ_{42}$, Ab42.2 capture and Ab9-HRP detection.

Immunohistology. Hemibrains of mice were fixed in 4% paraformaldehyde in 0.1 M PBS (pH 7.6) and then stained for Aβ plaques as described previously (2, 27). Paraffin sections (5 μm) were pretreated with 80% FA for 5 minutes, washed, and immersed in 0.3% H_2O_2 for 30 minutes to block intrinsic peroxidase activity. They were then incubated with 2% normal goat serum in PBS for 1 hour, with Ab9 (Monoclonal) at 1 μg/ml dilution overnight, and then with HRP-conjugated goat anti-mouse secondary mAb (1:500 dilution; Amersham Biosciences) for 1 hour. Sections were washed in PBS, and immunoreactivity was visualized by 3,3′-diaminobenzidine tetrahydrochloride (DAB) according to the manufacturer's specifications (ABC system; Vector Laboratories). Adjacent sections were stained with 4% thioflavin-S for 10 minutes. For cerebrovascular amyloid detection, paraffin sections were stained with biotinylated Ab9 mAb (1:500 dilution) overnight at 4°C, and then immunoreactivity was visualized by DAB according to the manufacturer's specifications (ABC system; Vector Laboratories). Positively stained blood vessels in the neocortex were visually assessed and divided into 3 groups based on the severity of CAA. Vessels with more than 80% of the perimeter stained were given the highest score (+++), partially stained vessels (30–80% stained) were given the median score (++), and only marginally stained vessels (less than 30% stained) were given the lowest score (+). Immunostained vessels were quantified in the neocortex of the same plane of section for each mouse (5–10 sections per mouse). Microhemorrhage in the vessels was assessed by staining of ferric iron with Perls staining according to a standard protocol and by H&E staining (24).

Quantitation of amyloid plaque burden. Computer-assisted quantification of Aβ plaques was performed using MCID Elite software (version 7.0; Imaging Research Inc.). Serial coronal sections stained as above were captured, and the threshold for plaque staining was determined and kept constant throughout the analysis. For analysis of plaque burdens in the passive immunization experiments, immunostained plaques were quantified (proportional area in old animals with vast deposition or plaque counts in young mice) in the neocortex of the same plane of section for each mouse (10–20 sections per mouse). In mice that were injected with mAb directly into the right hemisphere of the cortex, immunostained and thioflavin-S–stained plaques were quantified as above specifically in the vicinity of the injection site (2-mm × 2-mm block). A total of 6–10 injection sites per treatment group were used for quantitation. An additional series of 30 2-mm × 2-mm sites from the left hemispheres of cortices of mice that were not injected were also quantified and used as control values for amyloid plaque burden. All of the above analyses were performed in a blinded fashion.

Statistical analysis. One-way ANOVA followed by Dunnett's multiple comparison test was performed using the scientific statistic software Prism (version 3; GraphPad). *P* values less than 0.05 were considered significant.

Acknowledgments

These studies were funded by the NIH/National Institute on Aging (grant AG18454, to T.E. Golde). Additional resources from the Mayo Foundation, made possible by a gift from Robert and Clarice Smith, were used to support the Tg2576 mouse colony that provided the mice used in these studies. Y. Levites was supported by a John Douglas French Foundation fellowship. P. Das, M.P. Murphy, and Y. Levites were supported by a Robert and Clarice Smith Fellowship. We would like to thank David Westaway for providing us with breeding pairs of the CRND8 mice and Linda Rousseau, Virginia Phillips, and Monica Castanedes-Casey for technical assistance.

Received for publication April 19, 2005, and accepted in revised form October 18, 2005.

Address correspondence to: Todd E. Golde, Department of Neuroscience, Mayo Clinic Jacksonville, Birdsall 210, 4500 San Pablo Road, Jacksonville, Florida 32224, USA. Phone: (904) 953-2538; Fax: (904) 953-7370; E-mail: tgolde@mayo.edu.

Yona Levites and Pritam Das contributed equally to this work.

1. Das, P., et al. 2003. Amyloid-beta immunization effectively reduces amyloid deposition in FcRgamma–/– knock-out mice. *J. Neurosci.* **23**:8532–8538.
2. Hardy, J., and Selkoe, D.J. 2002. The amyloid hypothesis of Alzheimer's disease: progress and problems on the road to therapeutics. *Science.* **297**:353–356.
3. Iwatsubo, T., et al. 1994. Visualization of A beta 42(43) and A beta 40 in senile plaques with end-specific A beta monoclonals: evidence that an initially deposited species is A beta 42(43). *Neuron.* **13**:45–53.
4. Gravina, S.A., et al. 1995. Amyloid beta protein (A beta) in Alzheimer's disease brain. Biochemical and immunocytochemical analysis with antibodies specific for forms ending at A beta 40 or A beta 42(43). *J. Biol. Chem.* **270**:7013–7016.
5. Golde, T.E., Eckman, C.B., and Younkin, S.G. 2000. Biochemical detection of Abeta isoforms: implications for pathogenesis, diagnosis, and treatment of Alzheimer's disease. *Biochim. Biophys. Acta.* **1502**:172–187.
6. Klein, W.L., Stine, W.B., Jr., and Teplow, D.B. 2004. Small assemblies of unmodified amyloid beta-protein are the proximate neurotoxin in Alzheimer's disease. *Neurobiol. Aging.* **25**:569–580.
7. Walsh, D.M., and Selkoe, D.J. 2004. Oligomers on the brain: the emerging role of soluble protein aggregates in neurodegeneration. *Protein Pept. Lett.* **11**:213–228.
8. Younkin, S.G. 1998. The role of A beta 42 in Alzheimer's disease. *J. Physiol. (Paris).* **92**:289–292.
9. Jarrett, J.T., Berger, E.P., and Lansburry, P.T., Jr. 1993. The carboxy terminus of β amyloid protein is critical for the seeding of amyloid formation: implications for pathogenesis of Alzheimer's disease. *Biochemistry.* **32**:4693–4697.
10. Scheuner, D., et al. 1996. Secreted amyloid beta-protein similar to that in the senile plaques of Alzheimer's disease is increased in vivo by the presenilin 1 and 2 and APP mutations linked to familial Alzheimer's disease. *Nat. Med.* **2**:864–870.
11. Duff, K., et al. 1996. Increased amyloid-beta42(43) in brains of mice expressing mutant presenilin 1. *Nature.* **383**:710–713.
12. Games, D., et al. 1995. Alzheimer-type neuropathology in transgenic mice overexpressing V717F beta-amyloid precursor protein. *Nature.* **373**:523–527.
13. McGowan, E., et al. 2005. Abeta42 is essential for parenchymal and vascular amyloid deposition in mice. *Neuron.* **47**:191–199.
14. Iijima, K., et al. 2004. Dissecting the pathological effects of human Abeta40 and Abeta42 in Drosophila: a potential model for Alzheimer's disease. *Proc. Natl. Acad. Sci. U. S. A.* **101**:6623–6628.
15. Greeve, I., et al. 2004. Age-dependent neurodegeneration and Alzheimer-amyloid plaque formation in transgenic Drosophila. *J. Neurosci.* **24**:3899–3906.
16. Weggen, S., et al. 2001. A subset of NSAIDs lower amyloidogenic Abeta42 independently of cyclooxygenase activity. *Nature.* **414**:212–216.
17. Eriksen, J.L., et al. 2003. NSAIDs and enantiomers of flurbiprofen target γ-secretase and lower Aβ42 in vivo. *J. Clin. Invest.* **112**:440–449. doi:10.1172/JCI200318162.
18. Hsiao, K., et al. 1996. Correlative memory deficits, Abeta elevation, and amyloid plaques in transgenic mice. *Science.* **274**:99–102.
19. Kawarabayashi, T., et al. 2001. Age-dependent changes in brain, CSF, and plasma amyloid protein in the Tg2576 transgenic mouse model of Alzheimer's disease. *J. Neurosci.* **21**:372–381.
20. Wang, J., Dickson, D.W., Trojanowski, J.Q., and Lee, V.M. 1999. The levels of soluble versus insoluble brain Abeta distinguish Alzheimer's disease from normal and pathologic aging. *Exp. Neurol.* **158**:328–337.
21. Chishti, M.A., et al. 2001. Early-onset amyloid deposition and cognitive deficits in transgenic mice expressing a double mutant form of amyloid precursor protein 695. *J. Biol. Chem.* **276**:21562–21570.
22. Wilcock, D.M., et al. 2004. Passive immunotherapy against Abeta in aged APP-transgenic mice reverses cognitive deficits and depletes parenchymal amyloid deposits in spite of increased vascular amyloid and microhemorrhage. *J. Neuroinflammation.* **1**:24.
23. Kumar-Singh, S., et al. 2005. Dense-core plaques in Tg2576 and PSAPP mouse models of Alzheimer's

disease are centered on vessel walls. *Am. J. Pathol.* **167**:527–543.
24. Racke, M.M., et al. 2005. Exacerbation of cerebral amyloid angiopathy-associated microhemorrhage in amyloid precursor protein transgenic mice by immunotherapy is dependent on antibody recognition of deposited forms of amyloid beta. *J. Neurosci.* **25**:629–636.
25. Pfeifer, M., et al. 2002. Cerebral hemorrhage after passive anti-Abeta immunotherapy. *Science.* **298**:1379.
26. Odaka, A., et al. 2005. Passive immunization of the Abeta42(43) C-terminal-specific antibody BC05 in a mouse model of Alzheimer's disease. *Neurodegenerative Diseases.* **2**:36–43.
27. Bard, F., et al. 2003. Epitope and isotype specificities of antibodies to beta -amyloid peptide for protection against Alzheimer's disease-like neuropathology. *Proc. Natl. Acad. Sci. U. S. A.* **100**:2023–2028.
28. Das, P., Murphy, M.P., Younkin, L.H., Younkin, S.G., and Golde, T.E. 2001. Reduced effectiveness of Abeta1-42 immunization in APP transgenic mice with significant amyloid deposition. *Neurobiol. Aging.* **22**:721–727.
29. Das, P., and Golde, T.E. 2002. Open peer commentary regarding Abeta immunization and CNS inflammation by Pasinetti et al. *Neurobiol. Aging.* **23**:671–674; discussion 683–684.
30. Schenk, D. 2002. Amyloid-beta immunotherapy for Alzheimer's disease: the end of the beginning. *Nat. Rev. Neurosci.* **3**:824–828.
31. Lemere, C.A., et al. 2004. Alzheimer's disease abeta vaccine reduces central nervous system abeta levels in a non-human primate, the Caribbean vervet. *Am. J. Pathol.* **165**:283–297.
32. Schenk, D., et al. 1999. Immunization with amyloid-beta attenuates Alzheimer-disease-like pathology in the PDAPP mouse. *Nature.* **400**:173–177.
33. DeMattos, R.B., et al. 2001. Peripheral anti-A beta antibody alters CNS and plasma A beta clearance and decreases brain A beta burden in a mouse model of Alzheimer's disease. *Proc. Natl. Acad. Sci. U. S. A.* **98**:8850–8855.
34. Solomon, B. 2003. Immunological approach for the treatment of Alzheimer's disease. *J. Mol. Neurosci.* **20**:283–286.
35. Nitsch, R.M. 2004. Immunotherapy of Alzheimer disease. *Alzheimer Dis. Assoc. Disord.* **18**:185–189.
36. Wisniewski, T., and Frangione, B. 2005. Immunological and anti-chaperone therapeutic approaches for Alzheimer disease. *Brain Pathol.* **15**:72–77.
37. McLaurin, J., et al. 2002. Therapeutically effective antibodies against amyloid-beta peptide target amyloid-beta residues 4-10 and inhibit cytotoxicity and fibrillogenesis. *Nat. Med.* **8**:1263–1269.
38. Bussiere, T., et al. 2004. Morphological characterization of Thioflavin-S-positive amyloid plaques in transgenic Alzheimer mice and effect of passive Abeta immunotherapy on their clearance. *Am. J. Pathol.* **165**:987–995.
39. Chauhan, N.B., Siegel, G.J., and Feinstein, D.L. 2004. Effects of lovastatin and pravastatin on amyloid processing and inflammatory response in TgCRND8 brain. *Neurochem. Res.* **29**:1897–1911.
40. Oddo, S., Billings, L., Kesslak, J.P., Cribbs, D.H., and LaFerla, F.M. 2004. Abeta immunotherapy leads to clearance of early, but not late, hyperphosphorylated tau aggregates via the proteasome. *Neuron.* **43**:321–332.
41. Wilcock, D.M., et al. 2003. Intracranially administered anti-Abeta antibodies reduce beta-amyloid deposition by mechanisms both independent of and associated with microglial activation. *J. Neurosci.* **23**:3745–3751.
42. Hock, C., et al. 2003. Antibodies against beta-Amyloid slow cognitive decline in Alzheimer's disease. *Neuron.* **38**:547–554.
43. Gilman, S., et al. 2005. Clinical effects of Abeta immunization (AN1792) in patients with AD in an interrupted trial. *Neurology.* **64**:1553–1562.
44. Tycko, R., and Ishii, Y. 2003. Constraints on supramolecular structure in amyloid fibrils from two-dimensional solid-state NMR spectroscopy with uniform isotopic labeling. *J. Am. Chem. Soc.* **125**:6606–6607.
45. Nicoll, J.A., et al. 2003. Neuropathology of human Alzheimer disease after immunization with amyloid-beta peptide: a case report. *Nat. Med.* **9**:448–452.
46. Masliah, E., et al. 2005. Abeta vaccination effects on plaque pathology in the absence of encephalitis in Alzheimer disease. *Neurology.* **64**:129–131.
47. Bacskai, B.J., et al. 2002. Non-Fc-mediated mechanisms are involved in clearance of amyloid-beta in vivo by immunotherapy. *J. Neurosci.* **22**:7873–7878.
48. Chauhan, N.B., and Siegel, G.J. 2005. Efficacy of anti-Abeta antibody isotypes used for intracerebroventricular immunization in TgCRND8. *Neurosci. Lett.* **375**:143–147.
49. Fossati-Jimack, L., et al. 2000. Markedly different pathogenicity of four immunoglobulin G isotype-switch variants of an antierythrocyte autoantibody is based on their capacity to interact in vivo with the low-affinity Fcgamma receptor III. *J. Exp. Med.* **191**:1293–1302.
50. Orgogozo, J.M., et al. 2003. Subacute meningoencephalitis in a subset of patients with AD after Abeta42 immunization. *Neurology.* **61**:46–54.